Native and pregelatinized potato and rice starches and maltodextrin as encapsulating agents for linseed oil ethyl esters – comparison of emulsion and powder properties

Dorota Ogrodowska[1], Annelie Damerau[2], Paweł Banaszczyk[3], Małgorzata Tańska[1*], Iwona Z. Konopka[1], Beata Piłat[1], Fabian Dajnowiec[3], Kaisa M. Linderborg[2]

[1]Department of Food Plant Chemistry and Processing, Faculty of Food Sciences, University of Warmia and Mazury, Plac Cieszyński 1, 10-718, Olsztyn, Poland

[2]Food Sciences, Department of Life Technologies, University of Turku, 20014 Turun Yliopisto, Turku, Finland

[3]Engineering Department, Process Equipment and Food Biotechnology, Faculty of Food Sciences, University of Warmia and Mazury, Oczapowskiego 7, 10-719 Olsztyn, Poland

* Corresponding author.

E-mail address: m.tanska@uwm.edu.pl (M. Tańska)

Abstract

This study compared selected physical and chemical properties of emulsions and encapsulated powders containing linseed oil ethyl esters prepared with native and pregelatinized rice and potato starches, and potato maltodextrin. Emulsions with native starches and maltodextrin met the criteria of a Newtonian fluid, while with pregelatinized starches showed characteristics of a non-Newtonian fluid. The pregelatinized starches improved the emulsions' stability, yet emulsion degradation by creaming was comparable to that of emulsion containing maltodextrin. Only pregelatinized potato starch was characterized by increased encapsulation efficiency. Capsules made with both rice starches and native potato starch were

more oxidatively stable than that made with maltodextrin. Additionally, both powders with potato starch and pregelatinized rice starch showed a lower release of volatiles related to oxidation. Summarizing, pregelatinized potato starch displayed potential to replace maltodextrin based on relatively high encapsulation efficiency and high potential to diminish volatiles connected with oxidation processes, like hexanal.

Keywords

Encapsulation, Linseed oil, Ethyl esters, Oxidative stability, Starch, Volatile compounds

1. Introduction

Polyunsaturated fatty acids (PUFAs), especially from the omega-3 group, are essential nutrients in the human diet. In dietary supplements PUFA omega-3 are delivered mostly in the form of triacylglycerols (TAGs) or as ethyl esters (EEs). Health effects of fatty acids as EEs have generally not deviated from the health effects of fatty acids in TAGs, especially when ingested as part of fatty meals. It was stated that fish oil EEs diminish postprandial lipemia in familial hypercholesterolemia (Chan et al. 2017). Similarly, in statin-treated patients with high-sensitivity C-reactive protein ≥ 2.0 mg/L (a known biomarker of systemic inflammation) and TAGs from 200 to 499 mg/dL at baseline, eicosapentaenoic acid (EPA) EEs at a dose of 4 g/day significantly and safely reduced TAGs and other atherogenic and inflammatory parameters (Miller et al., 2019). In study conducted by Dogay Us and Mushtag (2022) diet supplementation with a dose of 4 g/day of EPA or docosahexaenoic acid (DHA) EEs improved subclass of various lipoproteins and TAGs to a greater extent than atorvastatin alone. All above mentioned studies confirm positive action of EPA and DHA fatty acids in the form of EEs, at a limited dose up to 4g/day on the human health. For this reason, fish EPA and DHA EEs

mixture was registered under the name of Omacor® (Rupp, 2009). This preparation increases the large and small artery elasticity in obese adults on a weight loss diet (Wong et al., 2013).

Food-derived sources of omega-3 PUFAs are primarily marine oils (fish, krill, algae) and some plant oils such as linseed, rapeseed, chia, and hemp oil (Ghasemifard et al., 2014; Saini et al., 2021). Plant sources of these fatty acids are crucial in vegetarians' and vegans' diet. One of the richest and easily available sources of omega-3 α-linolenic acid (ALA) is linseed oil. This oil usually contains above 50% of this fatty acid (Tańska et al., 2016).

Unfortunately, PUFAs can be easily oxidized through auto-, photo- or enzyme-catalysed oxidation. Encapsulation can protect the PUFAs against oxidation by shielding them against oxygen. Among known wall materials, various starches, and their preparations (like maltodextrin) are commonly used (Hoyos-Leyva et al., 2016; Ogrodowska et al., 2022). In the case of these materials, both the formation of wall and lipid-amylose complexes play a protective role.

Starch is a natural polymeric carbohydrate consisting of glucose units joined by α-1,4 and α-1,6 glycosidic bonds. It is formed by linear (amylose) and branched (amylopectin) molecules. In its native state, linear amylose in the presence of hydrophobic ligands, undergoes a conformational change resulting in a single, left-handed helix that can complex the ligand inside its inner cavity. This polymorphic form is known as V-type, with a variety of small ligands (Le-Bail et al., 2015; Gutierrez & Tovar, 2021). Based on their melting temperature, amylose-inclusion complexes are classified into types I or II. Type I is morphologically described as having a random distribution of the helical segments, whereas type II has an ordered semicrystalline structure and higher melting temperatures than type I. Self-assembled starch-lipid type I complexes are obtained by hydrophilic interactions (e.g., H-bonding) by using 12–18 carbon chain fatty acids, while type II complexes are generated via hydrophobic interactions (e.g., π interactions), by increasing the molecular weight of the fatty acid or by

using unsaturated fatty acids (more details in Gutierrez & Tovar, 2021). Starch/amylose inclusion complexes may be used as an appropriate preservation system for the delivery of different bioactive molecules that are sensitive to oxidation and heat. A wide variety of compounds have been complexed with amylose, such as fatty acid esters of vitamins, sterols, β-carotene, flavours, and ibuprofen, as well as monoacylglycerols (MAGs) and free fatty acids (FFAs) (Di Marco et al., 2020; Kong et al., 2019). It was suggested that starch-fatty acid complexes are organized in lamellae packed in submicron-sized spheroids, and that the spheroids form microscopic-sized aggregations (Gutierrez & Tovar, 2021).

Commercial starch preparations highly differ in origin and method of production (physical, chemical, enzymatic processing). Additionally, to date there is relatively little information on the use of various natural starches or their preparations for the encapsulation of PUFA-rich fatty acid mixtures, mainly ethyl esters of plant oils. Our recent study showed that during encapsulation, partly degraded commercial wheat starch could effectively capture tocopherols, squalene, and sterols, which resulted in diminishing the fatty acid deterioration in pumpkin oil (Ogrodowska et al., 2022). The novelty of current study is the use of linseed oil in the form of ethyl esters, which is more susceptible to formation of complexes with polysaccharide components of the coating material.

Therefore, the aim of this study was to compare selected physical and chemical properties of prepared emulsions and encapsulated powders containing linseed oil EEs prepared with the use of native and pregelatinized rice and potato starches, compared to maltodextrin used as the standard (control material) of typical wall matrix. The comparison was done based on emulsions (morphology, particle size distribution, stability, viscosity, and rheological properties) and powders (morphology, physicochemical properties, oxidative stability, and volatile compounds) properties. In the experiment, rice and potato starches were selected as being extremely different from each other, mainly in terms of morphological characteristics.

Potato starch granules have been observed to be oval and irregular or cuboidal in shape, with the average granule size in the range of 20 to 110 μm, while rice starch granules are angular-shaped and range from 3 to 5 μm in size. Also, potato starch has higher swelling power, solubility, paste clarity, and viscosity than rice and other cereal starches such as wheat and corn (Singh et al., 2003).

2. Materials and methods

2.1. Materials and Reagents

Linseed oil (LO) was purchased from the company "Olejarnia Świecie" (Świecie nad Osą, Poland). The fatty acid composition of the oil was as follows: C16:0 5.46 %, C18:0 2.79 %, C18:1(*n*-9) 19.19 %, C18:2(*n*-6) 16.24 %, C18:3(*n*-3) 54.66 %, and others 1.68 %, while its oxidative stability was 1.36 h (analysis was done according to the procedure described in work of Damerau et al., 2022). Starches were provided by Hortimex Company (Konin, Poland) with the following main characteristic:

R1 – native rice starch "Remy B7"; Beneo-Remy N.V. (Leuven-Wijgmaal, Belgium);

R2 – pregelatinized rice starch "Remy FGP"; Beneo-Remy N.V. (Leuven-Wijgmaal, Belgium);

P1 – native potato starch "Eliane 100"; Avebe U.A. (Veendom, The Netherlands);

P2 – pregelatinized potato starch "Eliane C100"; Avebe U.A. (Veendom, The Netherlands).

M – maltodextrin (DE = 17.5) as a comparative starch was used. It was purchased from Pepees S.A. Company (Łomża, Poland). The gum Arabic was purchased from Kremer Pigmente GmbH&Co.KG (Aichstetten, Germany).

Additionally, potassium hydroxide (KOH) and 96 % ethyl alcohol purchased from Chempur (Piekary Śląskie, Poland), and n-hexane purchased from Sigma-Aldrich (Poznań, Poland) were used in the study.

125

126 *2.2. Linseed oil ethyl esters (LEEs) production*

127 In the first stage of LEEs synthesis, a solution of alkaline catalyst in ethyl alcohol was
128 prepared (Armenta et al., 2007). For this purpose, 3 g of KOH in 400 mL of 96 % ethyl alcohol
129 in a 1000 mL flask was stirred at room temperature until complete dissolution. In the second
130 stage, 200 g of linseed oil was added to the alcohol mixture of KOH. The flask and contents
131 were refluxed at 76 °C for 2 h in a water bath. In the third stage, residual ethanol was removed
132 from the reaction mixture by distillation. After that, the reaction mixture was cooled to 20 °C
133 and washed three times with distilled water. The phases were each time separated using a
134 laboratory separatory funnel. In the final stage, the EEs were separated by centrifugation using
135 the MPV-350R laboratory centrifuge (MPW Med Instruments, Warsaw, Poland) at the
136 separation parameters of 15 min and 7130 x g. The LEEs were used to prepare the target
137 emulsion. Purity and lipid class of the end product was confirmed by thin layer chromatography
138 (data not shown).

139

140 *2.3. Target emulsion preparation*

141 The composition of the prepared emulsions was as follows: water (75 %), LEEs (10 %),
142 gum Arabic (7.5 %), and starches R1, R2, P1, P2 or maltodextrin (7.5 %). The proportion of
143 wall materials and LEE loading was established based on preliminary emulsion preparation
144 tests. Gum Arabic was used as an encapsulation agent due to its emulsifying properties. Its
145 aqueous dispersions exhibit excellent oil emulsifying properties, and emulsions containing it
146 have good stability. This is crucial in the stage of emulsion preparation in the spray drying
147 microencapsulation process. Furthermore, gum Arabic possesses very good film-forming
148 properties, which is significant for the stability of microencapsulated oil. Gum Arabic finds
149 wide application in microencapsulation processes since it is a cheap and easily available

polysaccharide (Patel & Goyal, 2015). The emulsion samples were prepared according to the following protocol. Firstly, the ingredients of the continuous phase (gum Arabic and each starch) were mixed with water (20 °C) using a Thermomix (Vorwerk, Germany) at 9000 rpm for 120 s to obtain a uniform dispersion of all components. Next, the LEEs as a dispersed phase ingredient were added (200 g per 1800 g of wall materials and water mixture), and mixing was continued to obtain an emulsion (mixing parameters were the same as previously). The resulting emulsion was additionally homogenized in two steps (first step at 24 MPa and second step at4 MPa) using a Panda 2K laboratory homogenizer (GEA Niro Soavi, Parma, Italy).

2.4. Microencapsulation process

The principles of the microencapsulation process using spray-drying are based on the scheme presented in the work of Bakry et al. (2015). The encapsulated LEEs were prepared using a pilot-plant spray-dryer (A/S Niro Atomizer, Copenhagen, Denmark). The spraying mechanism was a disc with a diameter of 110 mm and a revolution rate of 6400 rpm number. The drying parameters were controlled to keep an inlet temperature of 130 °C and outlet temperature of 90 °C, and the feed flow rate was 77 mL/min. The drying conditions were typical for the used equipment (recommended by producers) and had been previously adjusted during the encapsulation of pumpkin oil (Ogrodowska et al., 2022).

2.5 Scanning electron microscopy (SEM) imaging

Scanning electron microscopy (SEM Quanta 200; FEI Company, Hillsboro, OR) was used to visualize the morphology of maltodextrin, starches and LEEs powders. Samples were mounted on SEM stubs with the aid of two-sided adhesive tape and coated with palladium in a sputter coater. The samples were analysed at an accelerating voltage of 30 kV and 400× magnification.

175

176 *2.6. Particle size distribution analysis*

177 Particle sizes of starches, and LEEs emulsions and powders were determined by laser
178 diffraction analysis using Mastersizer 2000 (Malvern Instruments Ltd., Worcestershire, United
179 Kingdom). Additionally, the structure of the powders was described by Sauter mean diameter
180 $D_{3,2}$ (the surface weighted mean diameter), De Broucker mean diameter $D_{4,3}$ (the volume
181 weighted mean diameter), and specific surface area (SSA). The median size of the distribution
182 $d_{0.5}$, and $d_{0.1}$, $d_{0.9}$ (diameters of the droplets at which 10, 50 or 90 % of the sample is smaller
183 than the size measured, respectively) were used to calculate the width of the distribution (Span)
184 Eq. (1) (Malvern, 2007):

185 $$Span = \frac{d_{0.9} - d_{0.1}}{d_{0.5}} \quad \text{Eq. (1)}$$

186

187 *2.7. Emulsion microstructural analysis*

188 Microstructural analysis of the emulsions was conducted using a Motic BA210E with
189 Motic Camera 1080p optical microscope (Motic, Kowloon, Hong Kong) at a magnification of
190 40×.

191

192 *2.8. Emulsion stability analysis*

193 The stability of emulsion samples was determined using the turbidimetric method by
194 measuring the backscattering of light by Turbiscan Classic 2. The measurement was carried
195 out for 24 h with ΔRW registration every 5 min. Based on this, the profile of changes in the
196 backscattering coefficient (RW) over time was determined, and the slope coefficients of the
197 backscattering curve were calculated.

198

199 *2.9. Emulsion viscosity analysis*

The rheological properties were determined using a rheometer Rheolab QC Anton Paar. The range of applied shear rates was from 0 to 500 1/s. The measurement was conducted at a temperature of 21 ± 0.5 °C. For each sample, 100 measurement points were recorded.

2.10. Encapsulation efficiency analysis

Surface oil was extracted by mixing 2 g of LEE powder with 15 mL of n-hexane and shaking for 2 min at room temperature. The solvent was then filtered, and the collected solid residue was rinsed three times with 25 mL of n-hexane. The filtrate solution was evaporated using a rotary evaporator (Büchi Labortechnik AG, Switzerland). The residue was weighted, and the surface oil content was expressed as a percentage of the powder.

The encapsulation efficiency was calculated based on the following equation:

$$Encapsulation\ efficiency\ (\%) = \frac{(Total\ oil - Surface\ oil)}{Total\ oil} \cdot 100 \qquad \text{Eq. (2)}$$

where total oil was the total theoretical amount of oil in the powder calculated from the formulation.

2.11. Powder moisture analysis

The moisture content of the powders was measured according to the AOAC Official Method 925.10 (2000).

2.12. Oxidative stability analysis

A 743 Rancimat (Metrohm, Switzerland) eight-channel oxidative stability instrument was used to evaluate the oxidative stability index of LEEs and their powders (OSI; expressed in hours). A capped reaction vessel with a sample (2.5 g) was placed in a thermostatic electric heating block. The temperature was set at 110 °C, and an air flow rate of 20 L/h was applied.

225

226 *2.13. Volatile compound analysis*

227 Volatile compounds of linseed oil, LEEs non-encapsulated and encapsulated were
228 analysed according to the method of Damerau et al. (2014) with modifications. For the analysis,
229 0.3 g ± 0.006 g of oil and LEEs, and 0.5 g ± 0.010 g of powder was weighed in triplicate in 20-
230 mL headspace vials and flushed with nitrogen to prevent lipid oxidation during analysis.
231 Volatiles were extracted using headspace solid-phase microextraction (HS-SPME) using the
232 TriPlus RSH autosampler (Thermo Scientific, Switzerland) equipped with a
233 DVB/CAR/PDMS-fiber (50/30 μm film thickness; Supelco, USA). Extraction parameters:
234 incubation at 40 °C for 20 min, extraction at 40 °C for 30 min and desorption for 5 min at 240
235 °C. Volatiles were analysed with TRACE 1310 GC (Thermo Scientific) equipped with a DB-
236 WAX column (60 m, 0.25 mm, 0.25 μm; Agilent Technologies, Santa Clara, CA, USA) and
237 coupled with an ISQ 7000 mass spectrometer detector (Thermo Scientific). The GC-MS
238 operation conditions were as follows: helium flow 1.5 mL/min; GC oven 40 °C held 2 min, 4.5
239 °C/min to 110 °C, 2.0 °C/min to 130 °C, 3.0 °C/min to 160 °C, 5.0 °C/min to 225 °C and held
240 for 2 min; MS 70 eV, scan range 40 to 300 amu. Compounds were identified by using database
241 NIST MS Search library (NIST 20) (version 2.3. National Institute of Standards and
242 Technology, Gaithersburg, Maryland, USA). Data was processed with Chromeleon 7
243 Chromatography Data System Software (Thermo Fisher Scientific, Switzerland).

244

245 *2.14. Statistical analysis*

246 Data were analysed statistically using Statistica 13.3 (TIBCO Software Inc., Palo Alto,
247 CA, USA). The differences between the samples were determined using the one-way ANOVA
248 with Duncan's test. All analysed differences were considered statistically significant if the p-
249 value was below 0.05. Volatile compounds were analysed statistically using a one-way

ANOVA with Tukey WSD test in SPSS (IBM SPSS Statistics, version 25.0.0.1, IBM, New York, USA).

3. Results and Discussion

3.1. Effect of starch type on emulsion morphology and particle size distribution

Fig. 1 shows images of used starches and maltodextrin. As expected, native starches were characterized by a spherical structure, while pregelatinized starches were similar to flakes. The SEM images also show that the native rice starch (R1) was characterized by much smaller particles compared to the native potato starch (P1). $D_{0.5}$ of the main fraction for R1 was 6 μm, while for P1 it was 45 μm. It was additionally seen that R1 particles formed agglomerates. Chen et al. (2003) also observed that granules of rice starch had attached to each other after 60 min of ball-milling. This suggests that glycosidic bonds were broken during milling, increasing the number of free hydroxy groups to form hydrogen bonds between starch molecules (Li et al., 2014). Maltodextrin (M) SEM image (Fig. 1) was typical for this starch preparation, where different particle sizes can be observed with a spherical shape and rough surface resulting from different DE values and the drying process (Ogrodowska et al., 2022; Siemons et al., 2020; Alamilla-Beltrán et al., 2005).

Starches, maltodextrin, and gum Arabic were the wall materials used in the current experiment to prepare emulsions of the LEEs. The wall materials are absorbed in the interface between the aqueous and oil phases, resulting in lower surface tension, increased repulsion force, and prevention of droplet aggregation (Mahdi et al., 2022). Furthermore, the type and proportions of ingredients used as coating material (Mahdi et al., 2022) and homogenization parameters (Damerau et al., 2022) affect the emulsion droplet size. Mahdi et al. (2022) observed evident differences between the mean size diameter of droplets in the *Citrus*

reticulata essential oil (CREO) emulsions, which ranged from 352.85 to 664.74 nm. The whey protein-based CREO emulsion had the lowest diameter, while the highest value was found in the gum Arabic-based CREO emulsion. In contrast, combining whey protein with polysaccharides resulted in lower diameters than emulsions consisting of polysaccharides alone. On the other hand, in an experiment conducted by Damerau et al. (2022), the range of droplet diameters in the emulsion before the homogenization process was between 0.9 and 100 μm. The homogenization process significantly affected droplet size distribution, creating droplets in the range of 0.05–1 μm.

The image of the emulsion with R1 (Fig. 2) shows that its structure is not uniform, and the oil droplets tend to coalesce into larger aggregates. The interaction force between the droplets of the dispersed phase was not large because the aggregates disintegrated in the measuring cell during the analysis due to the mixing and circulation. The particle size distribution of emulsion with R1 was monomodal, with particles in the range of 1−15 μm. The image of emulsion with R2 shows a bimodal distribution of particles. A clearly dominant fraction is in the particle size range of 5.7–40 μm, while a small fraction of particles in the size range of 1−4.3 μm can also be observed. Droplets of the dispersed phase in emulsions containing pregelatinized starches do not tend to aggregate into clusters. The maintenance of dispersion of the oil phase can be explained by the alteration of the rheological properties of the dispersion system due to the addition of pregelatinized starch, which limited the migration of oil droplets, thus stabilizing the entire dispersion system (Dreher et al., 1999).

The particle size distribution of the emulsion with P1 is also bimodal (Fig. 2). The first fraction is in the range of 0.6–6.6 μm, while the second is in the range of 13.2–79.4 μm. Probably the first fraction is oil droplets, while the second fraction is starch granules, which is confirmed by the comparison of emulsion size distributions with the size distribution of native potato starch. Thus, large granules of starch were present in the emulsion after homogenization.

300 This thesis is supported by optical images of emulsion with P1, which show a fraction of the
301 emulsified oil phase and much larger granules of native potato starch (red loops). It is worth
302 nothing that a large fraction of starch shows a tendency to sediment (Saari et al., 2016).
303 As in the case of R2, in the microstructure of the emulsion with P2 there were two
304 fractions of oil droplets that differ in diameter. However, their sizes were not significantly
305 different from each other, therefore the existence of fraction of oil droplets with smaller
306 diameters can be seen in the figure of the particle size distribution as a breakdown of the
307 distribution curve and not a separate peak (Fig. 2), as is the case of emulsion with pregelatinized
308 rice starch (R2). The particle size distribution of the emulsion based on P2 indicates the
309 presence of one fraction of particles in the diameter range of 0.6–26 μm. However, the visible
310 breakdown of the distribution curve around 1 μm may imply the presence of a separate fraction
311 of smaller particles at this point.
312 The particle size distribution of the emulsion based on M (Fig. 2) indicates the presence
313 of one fraction of particles with diameter range of 0.48–6.6 μm. As in the case of LEE
314 emulsions with P2, the particle size distribution plot shows a kink in the small particle region,
315 indicating the presence of a separate particle fraction. Emulsions containing M and P1 were
316 emulsions in which the particle size of the dispersed phase of the main fraction was below 10
317 μm. The microscopic images reveal that droplets were evenly dispersed in space and did not
318 tend to form agglomerates.
319
320 *3.2. Effect of starch type on emulsion stability*
321 Turbidimetric analysis involves measuring the intensity of light reflected or transmitted
322 through a test sample. The light directed onto the sample is emitted in a pulsating manner, and
323 its detection is carried out by appropriate detectors (Lu et al., 2017). In the case of the analysed
324 emulsion samples, the transmitted light (transmittance) is very low, $T < 0.2$ (data not shown).

Therefore, stability analysis is based on backward scattering measurements. A sample is considered stable within the observed time when the determined profiles of backscattering values overlap, indicating uniform structure within the analysed area. This is also reflected in the value of the backscatter value (ΔRW) curve coefficient, which takes values close to zero for stable samples. Turbidimetric analysis of the stability of the emulsions showed that emulsions containing pregelatinized starches had relatively better stability than those made with native starches (Fig. 3). This is related to the presence of a separate fraction in emulsions containing native starches. In both cases, the graph of changes in the backscatter value (ΔRW) over time of emulsions containing native starches indicates a change in the emulsion structure associated with starch sedimentation and creaming of the oil phase that progressed during the measurement. However, in the case of the emulsion containing R1, the sedimentation process is the strongest, which can be related to the enhanced agglomeration ability of these small starch granules. Based on the graphs for emulsions containing R2, P2 and M, emulsion degradation by creaming is the smallest. The values of simple slopes RW suggest that, apart from the emulsion with M, the emulsion containing R2 was the most stable, despite the presence of relatively large droplets in the oil phase. Kim & Shin (2009) also used delta backscattering profiles to investigate the creaming stability of the emulsions. In their experiment, at the beginning of the scanning, the emulsion was homogeneous, but over time, ΔRW increased at the top part of the cylindrical glass cell and decreased at the bottom part. These results indicated that particle concentration at the top of the emulsion increased with particle migrations and that a subsequent cream layer was formed. This occurs because over time, the oil phase, having a lower density relative to the continuous phase of the emulsion, tends to concentrate in the upper layer of the measurement cell.

3.3. Effect of starch type on emulsion rheological properties

The rheological properties of an emulsion play a key role in both its stability and the encapsulation process. Different rheological characteristics can affect different aspects of these processes. The high viscosity of the emulsion allows stabilization of the dispersed phase, limiting its coalescence, which is later reflected in the uniform distribution of the core in the capsule matrix. Besides, viscosity influences the process of atomization of the feed in the drying chamber and the final size and shape of the capsule (Samavati et al., 2012). Emulsions containing native rice and potato starches and maltodextrin showed a constant value of the dynamic viscosity coefficient, independent of the change in the shear stress value. An example of the data for rice starch is shown in Fig. 4. Changes in the value of shear stress as a function of shear rate show that the emulsions met the criteria of a Newtonian fluid. The dynamic viscosity coefficient values for samples containing native starches (R1, P1) are at levels of 0.021 and 0.018 Pa s, respectively (Table 1). In turn, the viscosity of the sample containing M was at the lowest level (0.016 Pa s). This might be due to the high content of saccharides with a low polymerization degree in maltodextrin (Özbek & Ergönül, 2020).

In a study conducted by Mahdi et al. (2022) the viscosity values of gum Arabic, maltodextrin, and whey protein at a low shear rate were 0.087, 0.049, and 0.045 Pa·s and at a high shear rate were 0.024, 0.003, and 0.006 Pa·s, respectively. It was stated that maltodextrin reduces the emulsions' viscosity. According to Ang et al. (2021), the rheological properties of de-structured waxy potato starches were observed to change from shear-thickening, shear-thinning to Newtonian behaviour with increased treatment temperatures from 120 to 150 °C. Such behaviour contrasts with the shear-thinning behaviour observed in the gelatinized potato starch (95 °C).

Emulsions containing pregelatinized starches (R2 and P2) showed characteristics of a non-Newtonian fluid (Fig. 4). It can be seen that the shear stress decreases with increasing shear rate. Moreover, the emerging hysteresis loop indicates that the emulsions have

thixotropic properties but do not have a yield point (Ghica et al., 2016). The results were described using the rheological model of Ostwald de Waele, and the determined values of the coefficients are presented in Table 1. The consistency index (K) was lower in the sample containing R2 (0.32) compared to sample containing P2 (0.80). The opposite relation was observed in the case of the flow behaviour index (n), but these values are more uniform: 0.83 and 0.79, respectively (Table 1). The fitting coefficients of the measurement data to the Ostwald de Waele model were R^2 = 0.9998, indicating that the applied model accurately reflects the rheological properties of the tested sample. The absence of a yield point suggests that samples containing pregelatinized starches do not have the minimum stress value required to initiate flow. In the process of spraying thixotropic emulsions combined with their drying, as occurs in spray drying, the maximum shear force occurs during atomization, and at this point, the viscosity is the lowest. This can lead to the occurrence of secondary emulsion homogenization (Munoz-Ibanez et al., 2015), which affects encapsulation efficiency. There was no negative effect of the non-Newtonian nature of the R2 and P2 emulsions on powder properties. On the contrary, these powders were characterized by a lower surface oil content and thus a higher encapsulation efficiency. McMaster et al. (2005) reported that for successful encapsulation, the selected material should exhibit non-Newtonian properties i.e., be a relatively viscous material with solid properties.

In a study conducted by Özbek and Ergönül (2020), a mixture design with three components (20 % solid matter) was employed to evaluate the effects of whey proteins, maltodextrin, and gum Arabic on the rheological and physical properties of emulsions and some physicochemical characteristics of freeze–dried microcapsules. All the emulsions exhibited non–Newtonian behaviour. The viscosity of the emulsions decreased as the shear rate increased. The flow behaviour index (n) ranged between 0.36 and 0.46, which demonstrates that all the emulsions had shear-thinning (pseudoplastic) properties. Matsumura et al. (2000)

400 reported that a gum Arabic solution is considered to be a non-Newtonian fluid when its
401 concentrations is 18 % (w/w). Our study showed that non-Newtonian behaviour of fluid is
402 observed also at concentration of gum Arabic at 7.5 % with 7.5% of pregelatinized starches.
403
404 *3.4. Effect of starch type on powder morphology*
405 The powder images (Fig. 5) show spherical particles typical of spray-dried products
406 (Damerau et al., 2022; Sousa et al., 2022; Eztbach et al., 2020). On their surfaces are visible
407 cracks and pores, resulting from the fast water evaporation during the drying process and a
408 large number of small spots. According to Wagdare et al. (2011), these spots are oil droplets
409 enclosed within the polymer shell. Márquez-Gómez et al. (2018) observed these phenomena
410 during the spray-drying of orange essential oil using modified rice starch as wall material. In
411 their study, a spherical morphology of the microcapsules with a rough surface and high oil
412 content on the surface was found. In the current study, the powders with pregelatinized starches
413 (R2 and P2) were characterized by a greater number of particles with cracks, whereas the
414 powders with native starches (R1 and P1) and M had greater sphericity. Similar morphologies
415 of powders containing native rice starch (Ogrodowska et al., 2022) and maltodextrin
416 (Ogrodowska et al., 2017) were also observed previously.
417
418 *3.5. Effect of starch type on powder physicochemical properties*
419 Table 2 shows the physicochemical characteristics of powders. The moisture content was
420 the highest in the powder containing R1 (3.33 %) and the lowest in the sample with P1 (2.31
421 %). In our previous study (Ogrodowska et al., 2022), similar results were obtained for powders
422 containing native starches (2.40–3.11 %). Use of P1 as a wall component resulted in a powder
423 with the highest surface oil content (20.7 %). In turn, the use of P2 resulted in a low content of
424 surface oil in the powder (13.5 %). This dependence was not observed in the case of rice

starches (R1 and R2). In both samples, these levels were close to 16 % and were not statistically different ($p \leq 0.05$). The high differences between powders with native starches were probably the result of their pasting and solubility properties. Typically, potato starch is characterized by a higher pasting temperature (84.0 °C) and lower solubility at 40 °C compared to rice starch (65.2 °C) (Sánchez et al., 2010), which resulted in a lower covering of the core by the coating material with P1. The encapsulation efficiency is highly correlated ($r = -0.9989$) with the share of powder surface oil. Powder with P1, which contained the highest content of surface oil, was characterized by the lowest encapsulation efficiency (45.1 %). Pregelatinization of potato starch resulted in a significantly higher encapsulation efficiency (63.7 %). Such phenomena did not occur in rice starch. Márquez-Gómez (2018) also recommended rice starch as wall material is a viable alternative for encapsulation of essential oil because its high encapsulation efficiency. The highest encapsulation efficiency values (73.9 %) were found for powder made with M. Used maltodextrin has a relatively high dextrose equivalent of 17.5, indicating a high degree of depolymerization (Xiao et al., 2022), which can affect encapsulation efficiency results. Abd Ghani et al. (2017b) reported that encapsulation efficiency increased from 74 % to about 89 % on increasing DE values from 11 to 19. In their study, surface oil ratio for MD of DE = 11 was 26 % and almost two times that for DE = 19. Also, Campelo et al. (2017) confirmed better results for encapsulation efficiency when maltodextrin with higher DE was used. Furthermore, they found that a higher degree of hydrolysis of the maltodextrin chains (DE from 10 to 20) influenced particles with smoother surfaces and no visible fractures, which may protect the encapsulated material further.

The values of encapsulation efficiency obtained in the current study are similar to those presented by other authors. Firtin et al. (2020) used a mixture of maltodextrin and gum Arabic in a ratio of 1:1 as a coating material and obtained a powder characterized by an encapsulation efficiency of 67.4 %. According to Linke et al. (2020), an emulsion containing large droplets

450 results in a powder with a higher content of non-encapsulated oil. This phenomenon was
451 observed in the current study; the exception was only the powder containing P1. The high
452 content of surface oil, despite the relatively small emulsion droplets in this sample, may be due
453 to the difficulties that occurred during the homogenization of this emulsion, which resulted in
454 visible starch granules in optical images of the emulsion (Fig. 2). It follows that the coating
455 materials, with the exception of P1, probably form strong internal complexes with LEEs.
456 According to Tang and Copeland (2007), the lipid molecules can form complexes with amylose
457 or self-associate into micellar structures.

458 The powders with pregelatinized starches (R2 and P2) were characterized by a higher
459 surface weighted mean diameter ($D_{3,2}$) compared to powders containing native starch (R1 and
460 P1) (Table 2). The opposite relation was observed in the case of the volume weighted mean
461 diameter ($D_{4,3}$), where values were higher for powders containing native starches (R1 and P1).
462 In the case of rice starch, the results for the diameter $D_{4,3}$ were statistically indistinguishable
463 (ca. 110 μm). In contrast, the diameter $D_{4,3}$ of powders with potato starches highly differs, with
464 a value for P1 of 89.8 μm, while for P2 of 41.4 μm. The $D_{4,3}$ diameter and droplet size
465 distribution (Span) were at the highest level for the sample containing R1 (Table 2). The
466 specific surface area (SSA) varied from 0.18 (R2) to 0.29 m^2/g (M). SSA and Span values were
467 lower in powders made with pregelatinized starches (Table 2). This shows that particle size
468 was not directly correlated with emulsion viscosity. The results of Abd Ghani et al. (2017a)
469 suggest that higher encapsulation efficiency and lower surface oil content are achieved with
470 particles of larger diameters and smaller oil droplets in spray-dried powders. It may explain the
471 lower encapsulation efficiency of P1 powder with a smaller particle size compared to R1
472 powder.

473

474 *3.6. Effect of starch type on powder oxidative stability*

Linseed oil has a high content of *omega-3* α-linolenic acid (Tańska et al., 2016), which is easily oxidized due to the occurrence of three double bonds. Additionally, ethyl esters of oils are more susceptible to oxidation compared to oil, which is confirmed by the results presented in Fig. 6. The oxidation stability index (OSI) of LEEs was only 0.48 h. The encapsulation process increased the stability of LEEs by 2.3-3.1 times. Gallardo et al. (2013) microencapsulated linseed oil using maltodextrin and gum Arabic mixture as a coating material and determined an induction time of 3.8 h at 100 °C, which was 1.8 times higher compared to linseed oil. Pregelatinization of the starches increased OSI values, with the highest value for the powder with P2 (1.68 h). It can be seen in the case of potato starch that OSI values are related to the content of surface oil, since the lower oxidative stability exhibited powder containing P1 with higher content of surface oil compared to powder with P2 (Table 2). This phenomenon was previously confirmed in the study conducted by Drusch & Berg (2008). In turn, Ogrodowska et al. (2022) reported that oxidative stability was more dependent on carbohydrate wall material characteristics (ability to form a glassy shell that blocks surface pores, limiting oxygen diffusion toward the core material) than the surface oil content.

3.7. Volatile compounds of linseed oil (LO), LEEs and final powders

Twenty volatiles were identified in LO (Supplementary Table 1) with the HS-SPME-GC-MS method applied. The main volatiles detected were alcohols, followed by aldehydes, ketones, and furans. The most abundant volatile compound detected was 1-hexanol (*Z*). Identified volatiles have also previously been detected in linseed oils (Dlugogorski et al., 2012; Gómez-Cortés et al., 2015; Krist et al., 2006). The high number of alcohols compared to aldehydes is typical for cold pressed linseed oil, since heating will increase the number of aldehydes and other volatile secondary lipid oxidation compounds (Dlugogorski et al., 2012; Gómez-Cortés et al., 2015).

The volatile profile of LEEs compared to LO showed that the majority of volatiles of LO are lost in the ethyl esterification process, most likely due to the distillation step to remove residual ethanol and washing steps (Supplementary Table 1). While residual ethanol was removed, significant amounts of ethanol were still detected in LEEs. As ethanol was only a minor compound in the volatile profile of LO, it can be concluded that the ethanol detected in LEE is retained ethanol from the ethyl esterification process. Main compounds detected in both LEEs and LO were hexanal, 3-hydroxy-2-butanone, 1-hexanol (*Z*), 3,5-octadien-2-one (*E,Z/E,E*) and 2,3-butandiol. In addition to these, ethyl acetate, ethyl esters of short-chain fatty acids, and newly formed volatile secondary lipid oxidation compounds like 2,4-heptadienal (*E,Z/E,E*) were detected in LEEs as a result of the ethyl esterification process.

The volatile profiles of the spray-dried emulsions contained the same compounds as LEEs with the addition of terpenes originating from coating materials. Although a semi-quantitative comparison of the volatile profiles of LEEs and the spray-dried emulsion is difficult based on the differences in surface area and composition affecting the release of volatiles, it seems ethanol was further removed through spray-drying. Ethanol was most likely evaporated together with water in the drying process. To evaluate the effect of coating material on the release and retention of volatile compounds, peak areas of ethanol, hexanal, 3-hydroxy-2-butanone, 2,4-heptadienal (*E,Z/E,E*), and 3,5-octadien-2-one (*E,Z/E,E*) were compared. Ethanol was selected as its removal is desired. The other compounds are all originating from the encapsulated LEEs rather than from coating material. The highest retention of ethanol was seen for LEEs powder with P1, followed by powders with P2 and R2 (Fig. 7A). The lowest retention was seen for powders with M, which could be because of the smaller polymer size of M compared to the starches (Fig. 1). Low amounts of hexanal, 2,4-heptadienal (*E,Z/E,E*), and 3,5-octadien-2-one (*E,Z/E,E*) were detected for powders containing R2, P1, and P2, with no significant differences (Fig. 7B). For powder with P2, the amount of 3-hydroxy-2-butanone

525 was significantly higher than for powders with R2 and P1, although the lowest amounts were
526 found for those containing M and R1. 3-Hydroxy-2-butanone found naturally in foods is mainly
527 synthesized by microorganisms or higher plants (Xiao & Lu, 2014) and is therefore originating
528 from LO raw material in our study. While the hexanal, 2,4-heptadienal (*E,Z/E,E*), and 3,5-
529 octadien-2-one (*E,Z/E,E*) are typical volatile secondary lipid oxidation compounds of linseed
530 oil (Dlugogorski et al., 2012) and therefore could still be formed during the spray-drying
531 process. Therefore, the high levels detected in powder containing M, followed by powder
532 containing R1 of these volatiles could indicate either a higher release or oxidation of omega-3
533 fatty acid or both. This is consistent with the slightly lower value of OSI in samples with M
534 and R1 (Fig. 6). In general, lower detected volatiles are desired for flavour masking and
535 retarding oxidation; therefore, overall powder containing R2 performed the best, followed by
536 powders containing P1 and P2.
537
538 **4. Conclusions**
539 This study investigated the effect of starch type (native or pregelatinized) on the
540 properties of linseed oil ethyl ester emulsion and resulting powder produced by spray-drying.
541 The native starches used had spherical structures and were characterized by a smaller size,
542 while pregelatinized starches were similar to flakes. Additionally, the native potato starch was
543 characterized by much larger particles compared to the native rice starch, which resulted in the
544 obtaining the emulsion having a bimodal distribution of droplets. Although the dimensions of
545 droplets in emulsions containing native starches were generally smaller, the use of
546 pregelatinized starches improved the emulsion's stability, and emulsion degradation by
547 creaming was comparable to that of a control emulsion containing maltodextrin. Furthermore,
548 a non-Newtonian fluid characteristic was discovered in emulsions containing pregelatinized
549 starches, while emulsions with native starches met the criteria of a Newtonian fluid. Drying of

emulsion with pregelatinized potato starch resulted in significantly higher encapsulation efficiency in comparison to native potato starch and diminished surface oil content. Such effects were not observed for rice starch since both preparations were characterized by similar encapsulation efficiency and surface oil content. In general, native and pregelatinized rice starches and native potato starch were more efficient for oxidative stabilization of linseed oil ethyl ester powders than maltodextrin. The analysis of volatile compounds showed that all the starches used inhibited the formation of the typical volatile secondary linseed oil oxidation products. The powders with pregelatinized rice starch had the least pronounced release of volatiles, followed by powders with both types of potato starches. When overviewing all results, it was found that pregelatinized potato starch is good encapsulating agent for linseed oil ethyl esters, that can be used to replace maltodextrin. However, it is still possible to further optimise the emulsion preparation and/or spray-drying process conditions towards higher encapsulation efficiency and higher oxidative stability to increase the possible application of powders in food products such as yogurts, juices, drinks, infant formulas, or smoothies. Starch-based encapsulated oil can be successively employed in bakery and pastry products, enriching them with bioactive compounds, especially omega-3 fatty acids that are highly susceptible to oxidation. Starch-based encapsulation can also benefit in terms of masking specific flavour, and increasing water solubility of omega-3 sources, such as linseed, fish or microalgae oils or omega-3 concentrates.

Credit author statement

Dorota Ogrodowska: Conceptualization; Data curation; Formal analysis; Funding acquisition; Investigation; Methodology; Resources; Validation; Visualization; Writing – original draft; Writing – review & editing. Annelie Damerau: Formal analysis, Investigation, Writing – Original Draft, Writing – Review & Editing, Visualization, Supervision. Paweł Banaszczyk:

Formal analysis; Methodology; Writing – original draft. Małgorzata Tańska: Conceptualization; Formal analysis; Investigation; Methodology; Project administration; Resources; Visualization; Writing – original draft; Writing – review & editing. Iwona Z. Konopka: Conceptualization; Funding acquisition; Project administration; Writing – original draft; Writing – review & editing. Beata Piłat: Formal analysis. Fabian Dajnowiec: Formal analysis. Kaisa M. Linderborg: Resources, Writing – Review & Editing, Supervision, Project administration, Funding acquisition.

Acknowledgements

The work at University of Warmia and Mazury was financed from the "Rector's Scientific Grant" project. The work at University of Turku, Finland, was carried out with financial support from the Academy of Finland project "Omics of oxidation – Solutions for better quality of docosahexaenoic and eicosapentaenoic acids" (Decision No. 315274). The authors would like to thank Saida Samadova for technical assistance with part of the volatile analysis. The authors would like to thank Hortimex company for advising and providing starch samples.

Conflict of interest statement

Authors declare no conflicts of interest.

References

Abd Ghani, A., Adachi, S., Sato, K., Shiga, H., Iwamoto, S., Neoh, T.L., Adachi, S., Yoshii, H., 2017a. Effects of oil-droplet diameter and dextrose equivalent of maltodextrin on the surface-oil ratio of microencapsulated fish oil by spray drying. J. Chem. Eng. Japan 50 (10), 799–806. https://doi.org/10.1252/jcej.17we048

599 Abd Ghani, A., Adachi, S., Shiga, H., Neoh, T.L., Adachi, S., Yoshii, H., 2017b. Effect of
600 different dextrose equivalents of maltodextrin on oxidation stability in encapsulated fish
601 oil by spray drying. Biosci. Biotechnol. Biochem. 81 (4), 705–711.
602 https://doi.org/10.1080/09168451.2017.1281721
603 Alamilla-Beltrán, L., Chanona-Perez, J.J., Jimenez-Aparicio, A.R., Gutierrez-Lopez, G.F.,
604 2005. Description of morphological changes of particles along spray drying. J. Food Eng.
605 67 (1-2), 179–184. https://doi.org/10.1016/j.jfoodeng.2004.05.063
606 Ang, C.L., Matia-Merino, L., Lim, K., Goh, K.K.T., 2021. Molecular and physico-chemical
607 characterization of de-structured waxy potato starch. Food Hydrocoll. 117, 106667.
608 https://doi.org/10.1016/j.foodhyd.2021.106667
609 AOAC Official Method 925.10. Association of Official Analytical Chemists, 17th ed.; 2000.
610 Solids (total) and moisture in flour. Official Methods of Analysis: Gaithersburg, MD,
611 USA, 2000.
612 Armenta, R.E., Vinatoru, M., Burja, A.M., Kralovec, J.A., Barrow, C.J., 2007.
613 Transesterification of fish oil to produce fatty acid ethyl esters using ultrasonic energy.
614 J. Am. Oil Chem. Soc. 84 (11), 1045–1052. https://doi.org/10.1007/s11746-007-1129-2
615 Baker E.J., Miles E.A., Burdge G.C., Yaqoob P., Calder P.C., 2016. Metabolism and functional
616 effects of plant-derived omega-3 fatty acids in humans. Prog. Lipid Res. 64, 30–56.
617 https://doi.org/10.1016/j.plipres.2016.07.002
618 Bakry, A.M., Abbas, S., Ali, B., Majeed, H., Abouelwafa, M.Y., Mousa, A., Liang, L., 2015.
619 Microencapsulation of oils: A comprehensive review of benefits, techniques, and
620 applications. Compr. Rev. Food Sci. Food Saf. 15, 143–182.
621 https://doi.org/10.1111/1541-4337.12179
622 Campelo, P.H., do Carmo, E.L., Zacarias, R.D., Yoshida, M.I., Ferraz, V.P., de Barros
623 Fernandes, R.V., Botrel, D.A., Borges, S.V., 2017. Effect of dextrose equivalent on

624 physical and chemical properties of lime essential oil microparticles. Ind. Crops Prod.
625 102, 105–114. https://doi.org/10.1016/j.indcrop.2017.03.021
626 Carneiro, H.C., Tonon, R.V., Grosso, C.R., Hubinger, M.D., 2013. Encapsulation efficiency
627 and oxidative stability of flaxseed oil microencapsulated by spray drying using different
628 combinations of wall materials. J. Food Eng. 115 (4), 443–451.
629 https://doi.org/10.1016/j.jfoodeng.2012.03.033
630 Chan, D.C., Pang, J., Barrett, P.H.R., Sullivan, D.R., Burnett, J.R., van Bockxmeer, F.M.,
631 Watts, G.F., 2016. Ω-3 Fatty acid ethyl esters diminish postprandial lipemia in familial
632 hypercholesterolemia. J. Clin. Endocrinol. Metab. 101 (10), 3732–3739.
633 https://doi.org/10.1210/jc.2016-2217
634 Chen, J.J., Lii, C.Y., Lu, S.H.I.N., 2003. Physicochemical and morphological analyses on
635 damaged rice starches. J. Food Drug Anal. 11 (4), 10. https://doi.org/10.38212/2224-
636 6614.2684
637 Damerau, A., Kamlang-ek, P., Moisio, T., Lampi, A.-M., Piironen, V., 2014. Effect of SPME
638 extraction conditions and humidity on the release of volatile lipid oxidation products
639 from spray-dried emulsions. Food Chem. 157, 1–9,
640 https://doi.org/10.1016/j.foodchem.2014.02.032
641 Damerau, A., Ogrodowska, D., Banaszczyk, P., Dajnowiec, F, Tańska, F., Linderborg, K.M.,
642 2022. Baltic herring (*Clupea harengus membras*) oil encapsulation by spray drying using
643 a rice and whey protein blend as a coating material. J. Food Eng. 314, 110769.
644 https://doi.org/10.1016/j.jfoodeng.2021.110769
645 Di Marco, A.E., Ixtaina, V.Y., Tomás, M.C., 2020. Inclusion complexes of high amylose corn
646 starch with essential fatty acids from chia seed oil as potential delivery systems in food.
647 Food Hydrocoll. 108, 106030. https://doi.org/10.1016/j.foodhyd.2020.106030

Dlugogorski, J.B.Z., Kennedy, E.M., Mackie, J.C., 2012. Identification and quantitation of volatile organic compounds from oxidation of linseed oil. Ind. Eng. Chem. Res. 51 (16), 5645–5652. https://doi.org/10.1021/ie202535d

Dogay Us, G., Mushtaq, S., 2022. N-3 fatty acid supplementation mediates lipid profile, including small dense LDL, when combined with statins: a randomized double blind placebo controlled trial. Lipids Health Dis. 21, 84. https://doi.org/10.1186/s12944-022-01686-y

Dreher, T.M., Glass, J., O'Connor, A.J., Stevens, G.W., 1999. Effect of rheology on coalescence rates and emulsion stability. AIChE J. 45, 1182–1190. https://doi.org/10.1002/aic.690450604

Drusch, S., Berg, S., 2008. Extractable oil in microcapsules prepared by spray-drying: Localisation, determination, and impact on oxidative stability. Food Chem. 109(1), 17–24. https://doi.org/10.1016/j.foodchem.2007.12.016

Etzbach, L., Meinert, M., Faber, T., Klein, C., Schieber, A., Weber, F., 2020. Effects of carrier agents on powder properties, stability of carotenoids, and encapsulation efficiency of goldenberry (Physalis peruviana L.) powder produced by co-current spray drying. Curr. Res. Food Sci. 3, 73–81. https://doi.org/10.1016/j.crfs.2020.03.002

FAO-WHO. Fats and fatty acids in human nutrition: report of an expert consultation, FAO Food and Nutrition Paper #91, FAO, WHO: Geneva, Switzerland, 2010

Firtin, B., Yenipazar, H., Saygün, A., Şahin-Yeşilçubuk, N., 2020. Encapsulation of chia seed oil with curcumin and investigation of release behaivour & antioxidant properties of microcapsules during in vitro digestion studies. LWT-Food Sci. Technol. 134, 109947. https://doi.org/10.1016/j.lwt.2020.109947

671 Gallardo, G., Guida, L., Martinez, V., López, M.C., Bernhardt, D., Blasco, R., 2013.
672 Microencapsulation of linseed oil by spray drying for functional food application. Food
673 Res. Int. 52 (2), 473–482. https://doi.org/10.1016/j.foodres.2013.01.020
674 Ghasemifard, S., Turchini, G.M., Sinclair, A.J., 2014. Omega-3 long chain fatty acid
675 "bioavailability": A review of evidence and methodological considerations. Prog. Lipid
676 Res. 56, 92–108. https://doi.org/10.1016/j.plipres.2014.09.001
677 Ghica, M.V., Hîrjău, M., Lupuleasa, D., Dinu-Pîrvu, C.E., 2016. Flow and thixotropic
678 parameters for rheological characterization of hydrogels. Molecules 21(6), 786.
679 https://doi.org/10.3390/molecules21060786
680 Gómez-Cortés, P., Sacks, G.L., Brenna, J.T., 2015. Quantitative analysis of volatiles in edible
681 oils following accelerated oxidation using broad spectrum isotope standards. Food Chem.
682 174, 310–318. https://doi.org/10.1016/j.foodchem.2014.11.015
683 Gutiérrez, T.J., Tovar, J., 2021. Update of the concept of type 5 resistant starch (RS5): Self-
684 assembled starch V-type complexes. Trends Food Sci. Technol. 109, 711–724.
685 https://doi.org/10.1016/j.tifs.2021.01.078
686 Hoyos-Leyva, J.D., Bello-Pérez, L.A., Alvarez-Ramirez, J., Garcia, H.S., 2018.
687 Microencapsulation using starch as wall material: A review. Food Rev. Int. 34 (2), 148–
688 161. https://doi.org/10.1080/87559129.2016.1261298
689 Kim, D.Y., Shin, W.S., 2009. Roles of fucoidan, an anionic sulfated polysaccharide on BSA-
690 stabilized oil-in-water emulsion. Macromol. Res. 17, 128–132.
691 https://doi.org/10.1007/BF03218666
692 Kong, L., Perez-Santos, D.M., Ziegler, G.R., 2019. Effect of guest structure on amylose-guest
693 inclusion complexation. Food Hydrocolloids 97, 105188.
694 https://doi.org/10.1016/j.foodhyd.2019.105188

695 Krist, S., Stuebiger, G., Bail, S., Unterweger, H., 2006. Analysis of volatile compounds and
696 triacylglycerol composition of fatty seed oil gained from flax and false flax. Eur. J. Lipid
697 Sci. Technol. 108, 48–60. https://doi.org/10.1002/ejlt.200500267
698 Le-Bail, P., Houinsou-Houssou, B., Kosta, M., Pontoire, B., Gore, E., Le-Bail, A., 2015.
699 Molecular encapsulation of linoleic and linolenic acids by amylose using hydrothermal
700 and high-pressure treatments. Food Res. Int. 67, 223–229.
701 https://doi.org/10.1016/j.foodres.2014.11.003
702 Li, E., Dhital, S., Hasjim, J., 2014. Effects of grain milling on starch structures and flour/starch
703 properties. Starch-Stärke, 66 (1–2), 15–27. https://doi.org/10.1002/star.201200224
704 Linke, A., Weiss, J., Kohlus, R., 2020. Factors determining the surface oil concentration of
705 encapsulated lipid particles: impact of the emulsion oil droplet size. Eur. Food Res.
706 Technol. 246, 1933–1943. https://doi.org/10.1007/s00217-020-03545-5
707 Lu, Y., Kang, W., Jiang, J., Chen, J., Xu, D., Zhang, P., Feng, H., Wu, H., 2017. Study on the
708 stabilization mechanism of crude oil emulsion with an amphiphilic polymer using the β-
709 cyclodextrin inclusion method. RSC Adv. 7 (14), 8156–8166.
710 https://doi.org/10.1039/C6RA28528G
711 Mahdi, A.A., Mohammed, J.K., Al-Ansi, W., Al-Maqtari, Q.A., Al-Adeeb, A., Cui, H., Lin,
712 L., 2022. Stabilization of the oil‐in‐water emulsions of Citrus reticulata essential oil
713 by different combinations of gum arabic/maltodextrin/whey protein. J. Food Process.
714 Preserv. 46 (11), e16976, 1–12. https://doi.org/10.1111/jfpp.16976
715 Malvern, 2007. User Manual. Mastersizer 2000, MANO347. Issue 1.0. March 2007. Malvern
716 Instruments Ltd., Worcestershire, United Kingdom.
717 Márquez-Gómez, M., Galicia-García, T., Márquez-Meléndez, R., Ruiz-Gutiérrez, M.,
718 Quintero-Ramos, A., 2018. Spray-dried microencapsulation of orange essential oil using

719 modified rice starch as wall material. J. Food Process. Preserv. 42 (2), e13428.
720 https://doi.org/10.1111/jfpp.13428
721 Matsumura, Y., Satake, C., Egami, M., Mori, T., 2000. Interaction of gum arabic, maltodextrin
722 and pullulan with lipids in emulsions. Biosci. Biotechnol. Biochem. 64 (9), 1827–1835.
723 https://doi.org/10.1271/bbb.64.1827
724 McMaster, L.D., Kokott, S.A., 2005. Micro-encapsulation of Bifidobacterium lactis for
725 incorporation into soft foods. World J. Microbiol. Biotechnol. 21, 723–728.
726 https://doi.org/10.1007/s11274-004-4798-0
727 Miller, M., Ballantyne, C.M., Bays, H.E., Granowitz, C., Doyle Jr, R.T., Juliano, R.A., Philip,
728 S., 2019. Effects of icosapent ethyl (eicosapentaenoic acid ethyl ester) on atherogenic
729 lipid/lipoprotein, apolipoprotein, and inflammatory parameters in patients with elevated
730 high-sensitivity C-reactive protein (from the ANCHOR study). Am. J. Cardiol. 124 (5),
731 696–701. https://doi.org/10.1016/j.amjcard.2019.05.057
732 Munoz-Ibanez, M., Azagoh, C., Dubey, B.N., Dumoulin, E., Turchiuli, C., 2015. Changes in
733 oil-in-water emulsion size distribution during the atomization step in spray-drying
734 encapsulation. J. Food Eng. 167, 122–132.
735 https://doi.org/10.1016/j.jfoodeng.2015.02.008
736 Ogrodowska, D., Konopka, I.Z., Tańska, M., Brandt, W., Piłat, B., 2022. Effect of maltodextrin
737 replacement by selected native starches and disaccharides on physicochemical properties
738 of pumpkin oil capsules prepared by spray-drying. Appl. Sci. 12 (1), 33.
739 https://doi.org/10.3390/app12010033
740 Ogrodowska, D., Tańska, M., Brandt, W., 2017. The influence of drying process conditions on
741 the physical properties, bioactive compounds and stability of encapsulated pumpkin seed
742 oil. Food Bioproc. Tech. 10, 1265–1280. https://doi.org/10.1007/s11947-017-1898-z

743 Özbek, Z.A., Ergönül, P.G., 2020. Optimisation of wall material composition of freeze–dried
744 pumpkin seed oil microcapsules: Interaction effects of whey protein, maltodextrin, and
745 gum Arabic by D–optimal mixture design approach. Food Hydrocoll. 107, 105909.
746 https://doi.org/10.1016/j.foodhyd.2020.105909
747 Patel, S., Goyal, A., 2015. Applications of natural polymer gum arabic: A review. Int. J. Food
748 Prop. 18(5), 986–998. https://doi.org/10.1080/10942912.2013.809541
749 Rupp, H., 2009. Omacor®(prescription omega-3-acid ethyl esters 90): from severe rhythm
750 disorders to hypertriglyceridemia. Adv. Ther. 26, 675–690.
751 https://doi.org/10.1007/s12325-009-0045-2
752 Saari, H., Heravifar, K., Rayner, M., Wahlgren, M., Sjöö, M., 2016. Preparation and
753 characterization of starch particles for use in pickering emulsions. Cereal Chem. 93 (2),
754 116–124. https://doi.org/10.1094/CCHEM-05-15-0107-R
755 Saini, R.K., Prasad, P., Sreedhar, R.V., Akhilender Naidu, K., Shang, X., Keum, Y.-S., 2021.
756 Omega−3 polyunsaturated fatty acids (PUFAs): Emerging plant and microbial sources,
757 oxidative stability, bioavailability, and health benefits — A review. Antioxidants 10,
758 1627. https://doi.org/10.3390/antiox10101627
759 Samavati, V., Emam- Djomeh, J.Z., Mohammadifar, M.A., Omid, M., Mehdinia, A., 2012.
760 Application of rheological modeling in food emulsions. Iran. J. Chem. Chem. Eng. 31
761 (2), 71–83. https://doi.org/10.30492/ijcce.2012.5992
762 Sánchez, T., Dufour, D., Moreno, I.X., Ceballos, H., 2010. Comparison of pasting and gel
763 stabilities of waxy and normal starches from potato, maize, and rice with those of a novel
764 waxy cassava starch under thermal, chemical, and mechanical stress. J. Agric. Food
765 Chem. 58 (8), 5093–5099. https://doi.org/10.1021/jf1001606
766 Siemons, I., Politiek, R.G.A., Boom, R.M., Van der Sman, R.G.M., Schutyser, M.A.I., 2020.
767 Dextrose equivalence of maltodextrins determines particle morphology development

during single sessile droplet drying. Food Res. Int. 131, 108988. https://doi.org/10.1016/j.foodres.2020.108988

Singh, N., Singh, J., Kaur, L., Sodhi, N.S., Gill, B.S. 2003. Morphological, thermal and rheological properties of starches from different botanical sources. Food Chem. 81 (2), 219–231. https://doi.org/10.1016/S0308-8146(02)00416-8

Sousa, V.I., Parente, J.F., Marques, J.F., Forte, M.A., Tavares, C.J. 2022. Microencapsulation of essential oils: A review. Polymers 14(9), 1730. https://doi.org/10.3390/polym14091730

Tang, M.C., Copeland, L., 2007. Analysis of complexes between lipids and wheat starch. Carbohydr. Polym. 67 (1), 80–85. https://doi.org/10.1016/j.carbpol.2006.04.016

Tańska, M., Roszkowska, B., Skrajda, M., Dąbrowski, G., 2016. Commercial cold pressed flaxseed oils quality and oxidative stability at the beginning and the end of their shelf life. J. Oleo Sci. 65 (2), 111–121. https://doi.org/10.5650/jos.ess15243

Wagdare, N.A., Marcelis, A.T., Boom, R.M., van Rijn, C.J., 2011. Microcapsules with a pH responsive polymer: influence of the encapsulated oil on the capsule morphology. Colloids Surf. B: Biointerfaces 88 (1), 175–180. https://doi.org/10.1016/j.colsurfb.2011.06.028

Wang, D.H., Yang, Y., Wang, Z., Lawrence, P., Worobo, R.W., Brenna, J.T., 2019. High levels of branched chain fatty acids in nātto and other Asian fermented foods. Food Chem. 286, 428–433. https://doi.org/10.1016/j.foodchem.2019.02.018

Wong, A.T., Chan, D.C., Barrett, P.H.R., Adams, L.A., Watts, G.F., 2013. Supplementation with n3 fatty acid ethyl esters increases large and small artery elasticity in obese adults on a weight loss diet. J. Nutr. 143 (4), 437–441. https://doi.org/10.3945/jn.112.169359

Xiao, Z., Lu, J.R., 2014, Generation of acetoin and its derivatives in foods. J. Agric. Food Chem. 62 (28), 6487–6497. https://doi.org/10.1021/jf5013902

793 Xiao, Z., Xia, J., Zhao, Q., Niu, Y., Zhao, D., 2022. Maltodextrin as wall material for
794 microcapsules: A review. Carbohydr. Polym. 120113.
795 https://doi.org/10.1016/j.carbpol.2022.120113

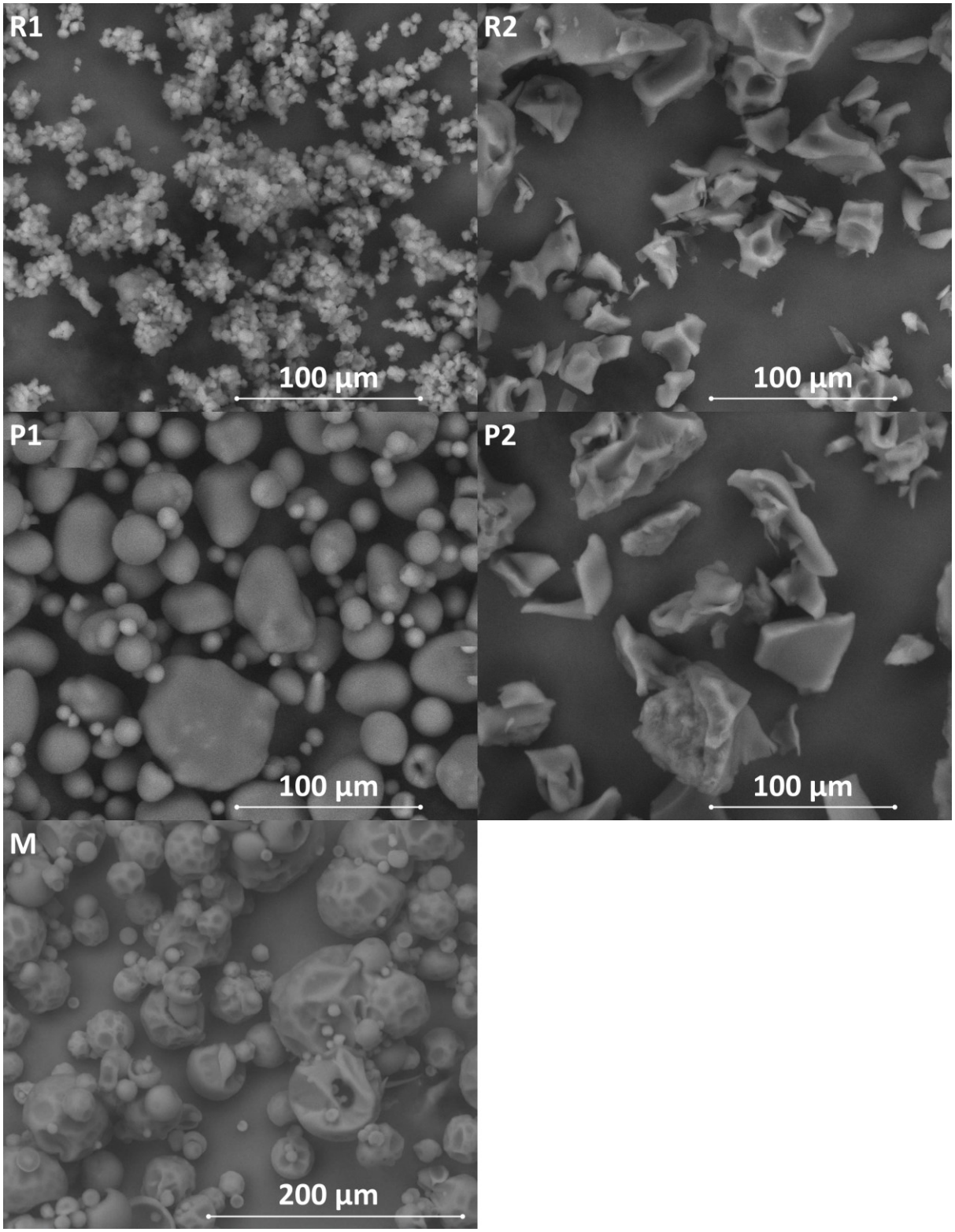

796

797 **Fig. 1.** SEM images of native rice starch (R1), pregelatinized rice starch (R2), native potato

798 starch (P1), pregelatinized potato starch (P2), and maltodextrin (M).

799

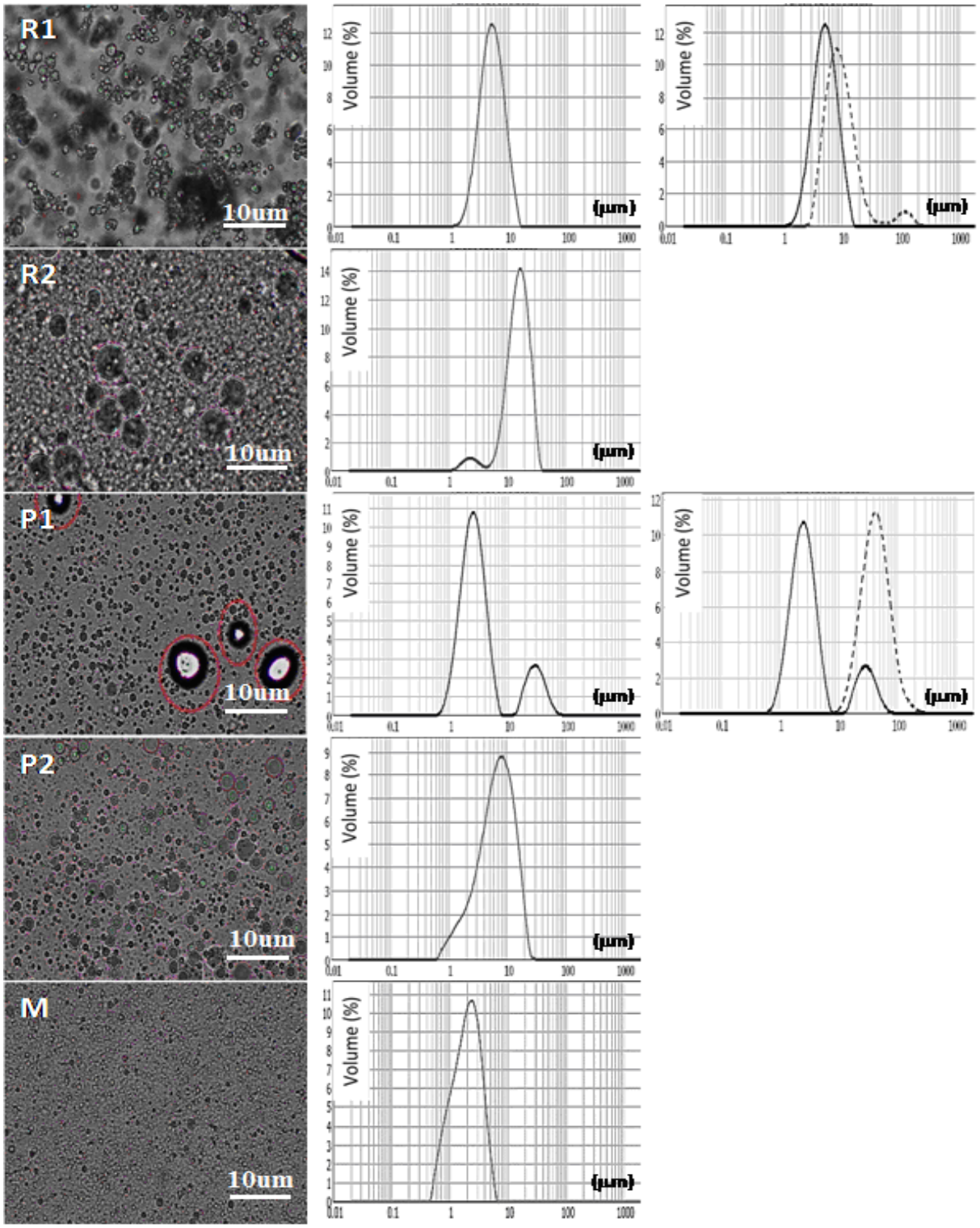

Fig. 2. Optical microscope images (red loop – starch grains, magnification 40×) and particle size distribution (solid line – emulsion, the dotted line – unhomogenized starch "background") in LEEs emulsions with native rice starch (R1), pregelatinized rice starch (R2), native potato starch (P1), pregelatinized potato starch (P2), and maltodextrin (M).

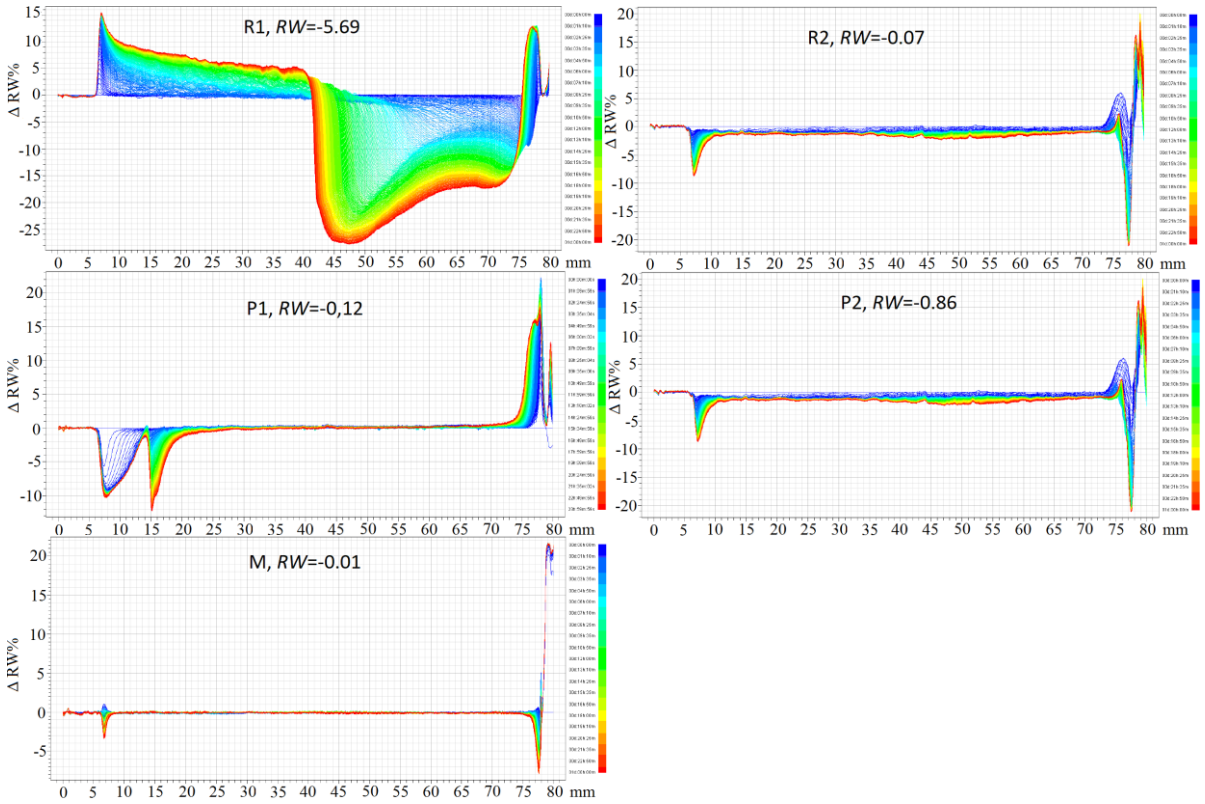

Fig. 3. Changes in the backscattering of light (*ΔRW*), and backscattering coefficient (RW) in the height range of 7–70 mm observed for LEEs emulsions with native rice starch (R1), pregelatinized rice starch (R2), native potato starch (P1), pregelatinized potato starch (P2), and maltodextrin (M). The lines of different colours represented the changes in the light back scattering over time.

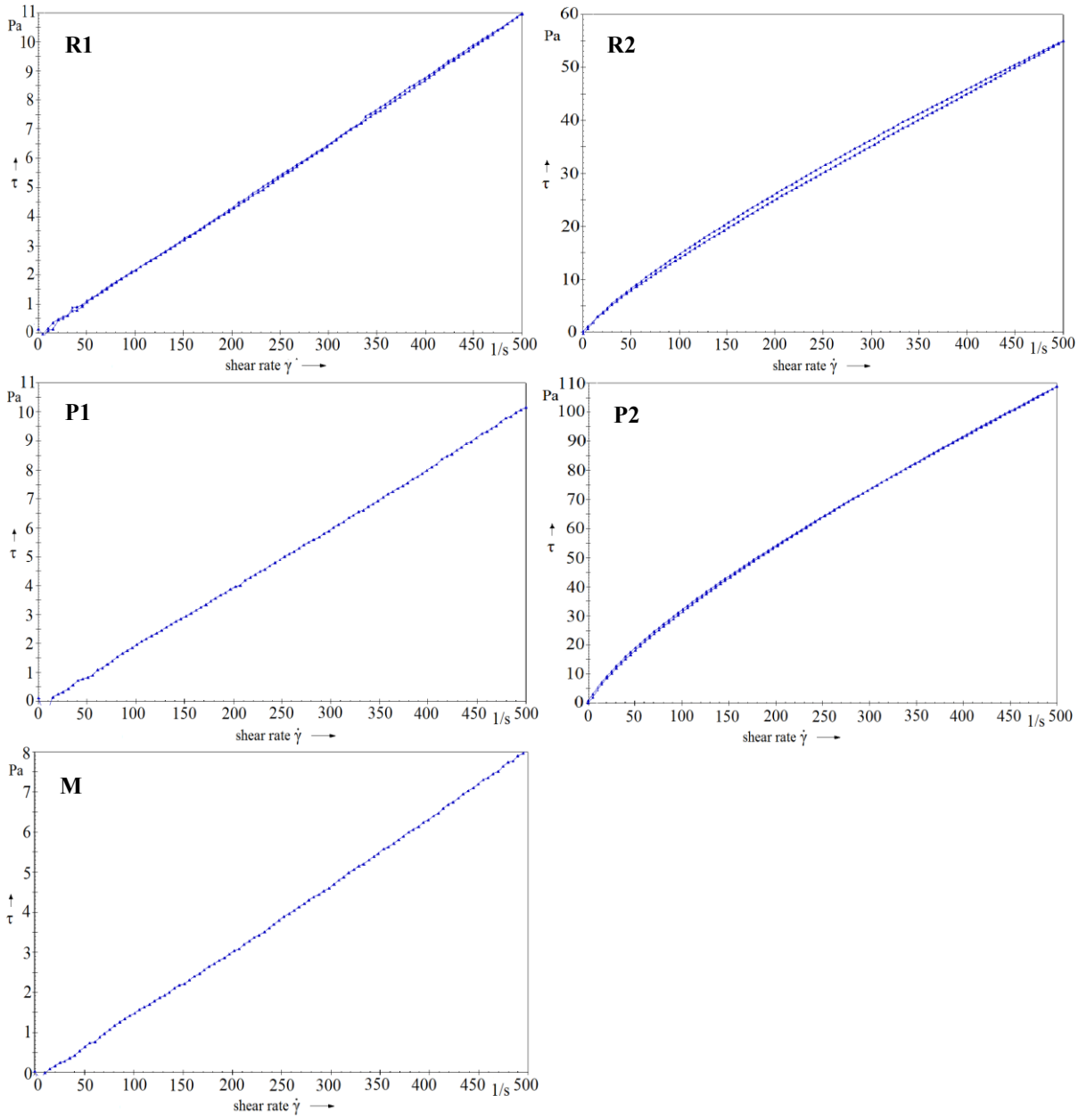

Fig. 4. Changes in the value of shear stress (τ) as a function of shear rate ($\dot{\gamma}$) of an emulsion containing native rice starch (R1) and pregelatinized rice starch (R2).

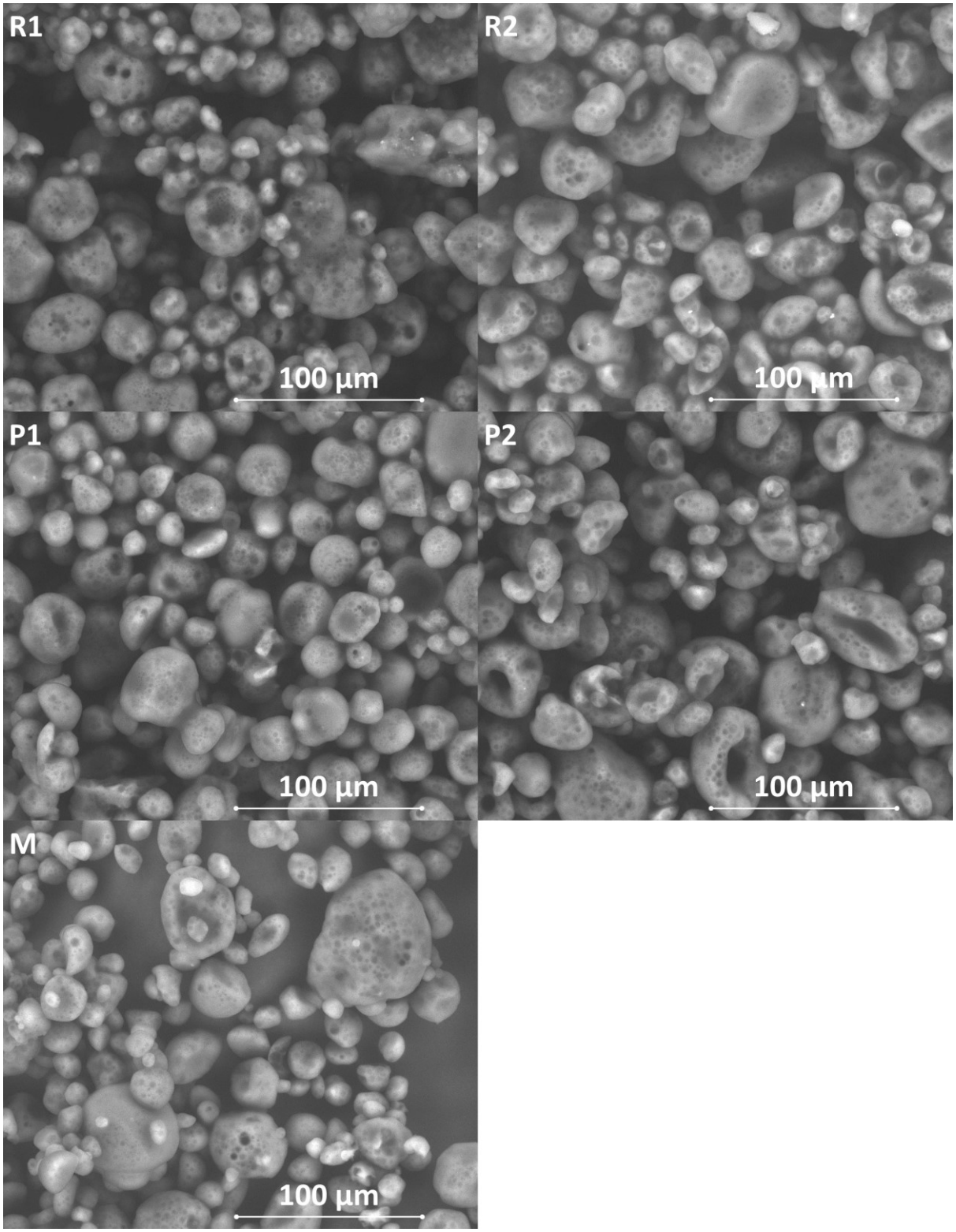

821

822 **Fig. 5.** SEM images of LEE powders with native rice starch (R1), pregelatinized rice starch

823 (R2), native potato starch (P1), pregelatinized potato starch (P2), and maltodextrin (M).

824

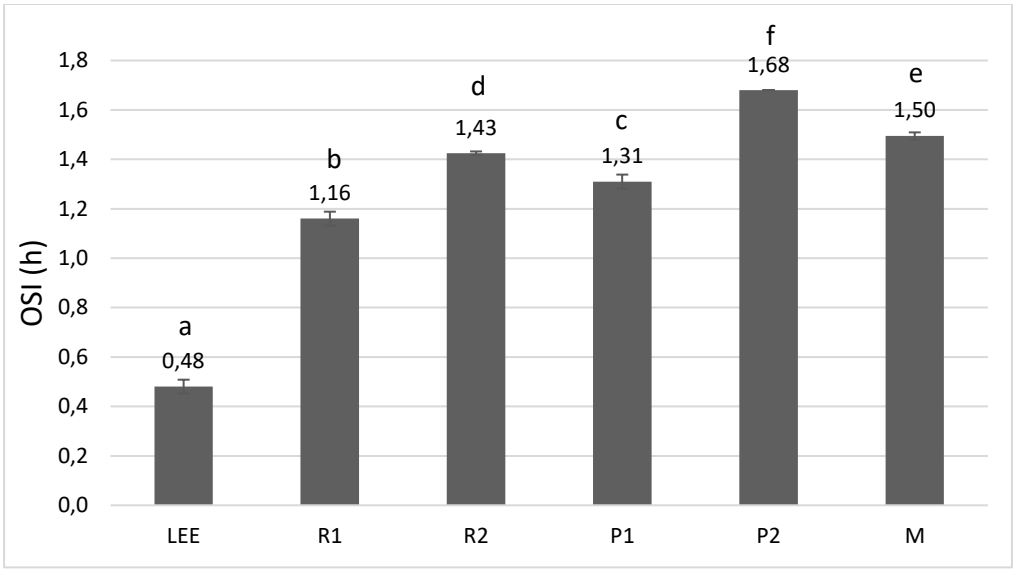

825

826 **Fig. 6.** Oxidative stability index of LEE and LEES powders with native rice starch (R1),
827 pregelatinized rice starch (R2), native potato starch (P1), pregelatinized potato starch (P2), and
828 maltodextrin (M). All values are mean ± standard deviation (n = 3). Means with different letters
829 are significantly different ($p < 0.05$).

830

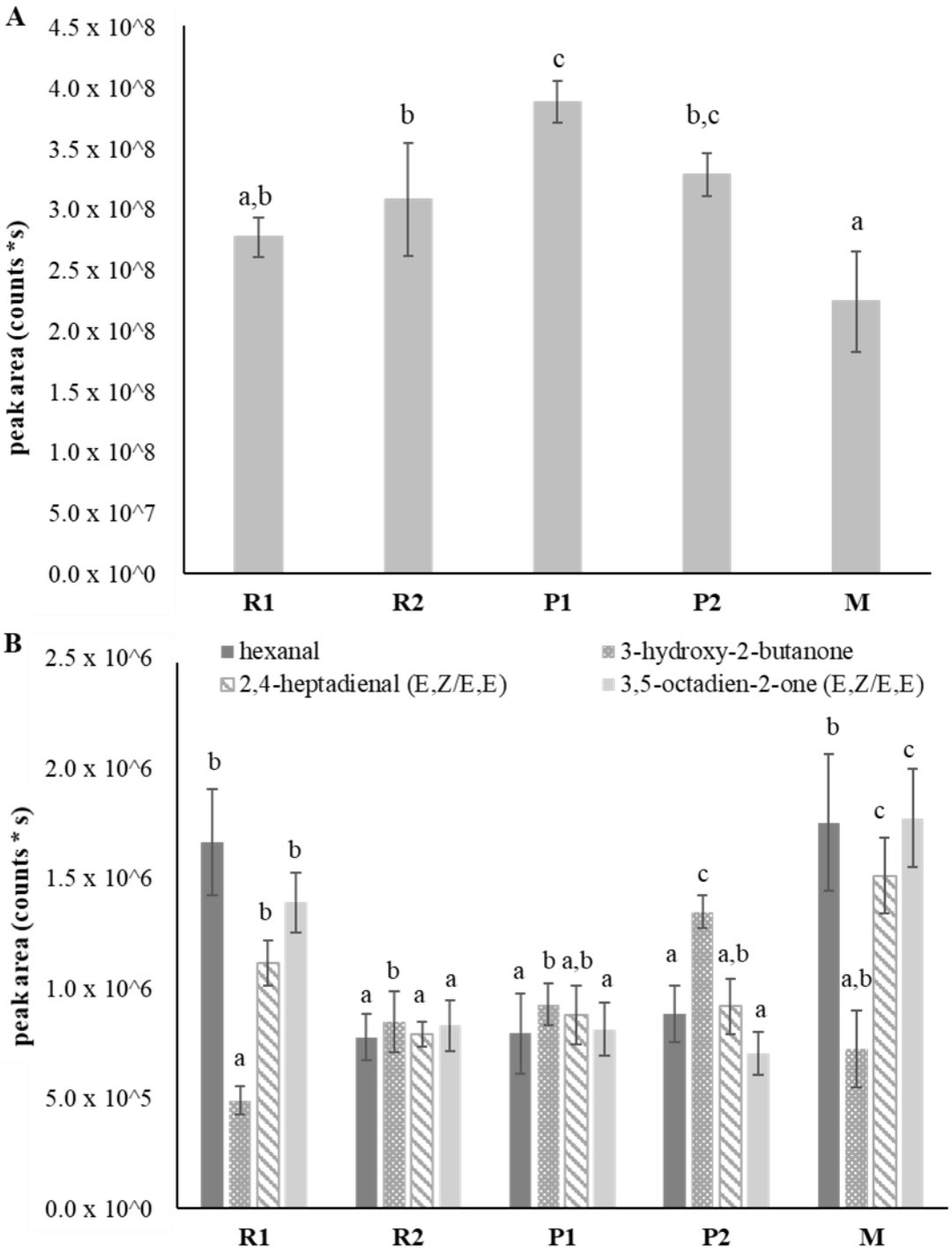

Fig. 7. Peak area data (n = 3) of ethanol (**A**), and hexanal, 3-hydroxy-2-butanone, 2,4-heptadienal (*E,Z/E,E*) and 3,5-octadien-2-one (*E,Z/E,E*) (**B**) in LEEs powders with native rice starch (R1), pregelatinized rice starch (R2), native potato starch (P1), pregelatinized potato starch (P2), and maltodextrin (M). Different letters above bars indicate a statistically significant difference ($p < 0.05$) between peak areas of different powders for each volatile compound.

837 **Table 1.** Characteristics of viscosity, consistency index (K) and flow behaviour index (n) of
838 LEEs emulsions.

	R1	R2	P1	P2	M
Viscosity (Pa s)	0.021 ± 0.01	- n.a.	0.018 ± 0.01	- n.a.	0.016 ± 0.01
K	n.a.	0.32 ± 0.01	- n.a.	0.80 ± 0.02	- n.a.
n	- n.a.	0.83 ± 0.01	- n.a.	0.79 ± 0.01	- n.a.

839 LEES emulsions with native rice starch (R1), pregelatinized rice starch (R2), native potato starch (P1),
840 pregelatinized potato starch (P2), and maltodextrin (M). n.a. – not analysed (parameters dependent on rheological
841 characteristics of emulsion which exhibits thixotropic properties). All values are mean ± standard deviation (n =
842 6).
843

844

845 **Table 2.** Physicochemical properties of LEEs powders.

	R1	R2	P1	P2	M
Moisture (%)	3.33 ± 0.26^{d}	3.09 ± 0.10^{c}	2.31 ± 0.21^{a}	2.79 ± 0.09^{b}	2.49 ± 0.05^{a}
Surface oil (%)	16.3 ± 0.49^{c}	15.9 ± 0.05^{c}	20.7 ± 0.71^{d}	13.5 ± 0.34^{b}	9.8 ± 0.46^{a}
Encapsulation efficiency (%)	55.63 ± 0.73^{b}	56.82 ± 0.18^{b}	45.08 ± 1.11^{a}	63.69 ± 0.70^{c}	73.90 ± 0.90^{d}
$D_{3,2}$ (μm)	27.6 ± 0.33^{c}	32.9 ± 1.34^{e}	25.9 ± 1.09^{b}	29.6 ± 0.32^{d}	20.9 ± 0.36^{a}
$D_{4,3}$ (μm)	110.1 ± 14.03^{c}	106.5 ± 8.72^{c}	89.8 ± 9.93^{b}	41.4 ± 0.29^{a}	96.4 ± 8.17^{b}
Span (-)	6.08 ± 0.82^{e}	3.41 ± 0.37^{c}	2.42 ± 0.19^{b}	1.68 ± 0.06^{a}	4.38 ± 0.27^{d}
SSA (m^2/g)	0.22 ± 0.00^{c}	0.18 ± 0.00^{a}	0.23 ± 0.01^{d}	0.20 ± 0.00^{b}	0.29 ± 0.01^{e}

846 LEEs powders with native rice starch (R1), pregelatinized rice starch (R2), native potato starch (P1),
847 pregelatinized potato starch (P2), and maltodextrin (M). D3,2 – Sauter mean diameter (the surface weighted mean
848 diameter, De Broucker mean diameter D4,3 (the volume weighted mean diameter), SSA – specific surface area.
849 All values are mean ± standard deviation (n = 6). Means within a row with different letters are significantly
850 different ($p < 0.05$).

851

852 **Supplementary Table 1**

853 Retention times, Kováts retention index, match with NIST Mass Spectral Library (NIST 20;
854 perfect match with spectra of pure compound is 1000) and main ions in the MS-spectra of 20
855 identified volatile compounds analysed from linseed oil.

	Compound	Retention time [min]	Kováts retention index	Match with NIST20	Main ions [*m/z*]
1	2-methylfuran	5.90	896	874	53, 70, 82
2	3-methylbutanol	6.33	919	851	44, 85, 71, 86
3	ethanol*	6.80	941	932	45
4	2-ethylfuran	7.06	953	864	53, 67, 81, 96
5	2-butanol	8,96	1032	954	45, 49, 73
6	1-propanol	9.33	1046	935	42, 59
7	hexanal*	10.43	1083	967	44, 56, 67, 72, 82
8	2-methyl-1-propanol	10.79	1096	907	43, 55, 74
9	3-pentanol	11.27	1113	944	41, 43, 57, 59
10	1-penten-3-ol	12.85	1164	917	57, 67, 86
11	3-methyl-1-butanol	14.37	1209	936	41, 55, 70
12	2-hexenal (*E*)	14.66	1219	947	41, 55, 69, 83, 98
13	1-pentanol	15.70	1254	960	42, 55, 57. 70
14	3-hydroxy-2-butanone*	16.84	1289	890	45, 53, 73, 88
15	1-hexanol*	18.90	1354	952	43, 45, 56, 69
16	3-hexen-1-ol (*Z*)	19.95	1386	954	41, 53, 55,67, 82, 100
17	3-octanol	20.19	1393	913	41, 59, 69, 83, 101. 112
18	3,5-octadien-2-one (*E,Z/E,E*)*	24.90	1521	886	53, 67, 81, 95, 109, 124
19	2,3-butanediol*	27.42	1583	970	43, 45, 57, 75, 90
20	γ-butyrolactone	29.54	1635	947	42, 56, 86

856 * volatile compounds also identified in linseed oil ethyl esters